Check for updates

ADVANCED MATERIALS TECHNOLOGIES
www.advmattechnol.de

Design of Blood Vessel Models using Magnetic-Responsive Vascular Platforms

Ana C. Manjua, Joaquim M.S. Cabral, Frederico Castelo Ferreira, Han Gardeniers, Carla A.M. Portugal, and Burcu Gumuscu**

The design of physiologically relevant blood vessel in vitro models has been impaired by the difficulty to reproduce the complex architecture of native blood vessels and the mechanisms mediating key cellular functions within miniaturized perfusable systems. Aiming to simulate blood vessel walls, in this work innovative 2D platforms are designed and patterned with magnetic-responsive gelatin for enabling in situ co-culture of mesenchymal stromal cells (MSCs) and human umbilical vein endothelial cells (HUVECs) within confined compartments. The performance of the 2D chips is evaluated based on HUVECs migration, adherence, and angiogenic behavior (proliferation and sprouting), as well as production of Endothelin-1 (endothelium marker), and compared with the results of 3D single channel models, designed to mimic the morphology of native arteries and veins. The 2D chips obtain better cell adhesion and angiogenic performance, which is attributed to flow profiles and VEGF concentration gradients. Magnetic stimulation is then used as a novel strategy to increase cell sprouting and endothelization ≈1.5 times above the control condition. These bio-inspired devices advance the exploration of magnetism for a finer convergence to the native vascular conditions in vitro and improved modulation of angiogenesis, showing promising contributions to the development of sophisticated therapeutics for vascular ischemia-related diseases.

1. Introduction

Vascular diseases are ranked among the disorders with the highest morbidity worldwide, accounting for poor knowledge of the diseases and inadequate therapeutic approaches.[1] Current therapeutic programs relying on animal models are not able to efficiently predict human pathophysiology and drug responses.[2] Additionally, the process of mimicking a patient's native blood vessel architecture remains challenging, hindering the development of novel treatment strategies. The wide variation of blood vessels' diameters, ranging from a few millimeters to micrometers, increases drastically the complexity of replicating native blood vessel networks.[3,4]

Traditionally in vitro platforms relied on endothelial cells (ECs) growing on coated 2D surfaces with adhesive proteins or spheroids of ECs within 3D hydrogel scaffolds encapsulated with specific growth factors such as VEGF-A.[5] Although these models offered insight into vessel assembly, they could not simultaneously introduce both chemical and mechanical stimuli in adequate spatiotemporal conditions.[6] Acknowledging these hurdles, tissue-engineered constructs (e.g., synthetic materials, biological scaffolds, porous hydrogels, fibrous meshes) with changeable properties have been developed to prompt cell adhesion, migration, and proliferation.[7]

A. C. Manjua, C. A. Portugal
LAQV-REQUIMTE
Department of Chemistry
NOVA School of Science and Technology, Universidade Nova de Lisboa
Campus da Caparica
2829-516 Caparica, Portugal
E-mail: a.c.baeta.manjua@tue.nl; cmp@fct.unl.pt

A. C. Manjua, J. M. Cabral, F. C. Ferreira
Department of Bioengineering and iBB – Institute for Bioengineering and Biosciences
Instituto Superior Técnico
Universidade de Lisboa, Av. Rovisco Pais
1049-001 Lisboa, Portugal

J. M. Cabral, F. C. Ferreira
Associate Laboratory i4HB – Institute for Health and Bioeconomy
Instituto Superior Técnico
Universidade de Lisboa
Lisboa 1049-001, Portugal

H. Gardeniers, B. Gumuscu
Mesoscale Chemical Systems Group
MESA+ Institute
University of Twente
Enschede 7500 AE, The Netherlands
E-mail: b.gumuscu@tue.nl

B. Gumuscu
Biosensors and Devices Lab
Biomedical Engineering Department
Institute for Complex Molecular Systems
Eindhoven Artificial Intelligence Systems Institute
Eindhoven University of Technology
Eindhoven 5600 MB, The Netherlands

The ORCID identification number(s) for the author(s) of this article can be found under https://doi.org/10.1002/admt.202300617

DOI: 10.1002/admt.202300617

 © 2023 Wiley-VCH GmbH

Advances in microfluidic design have also brought uncountable advantages to the study of cardiovascular biomechanics, including the ability to (1) control the flow at physiological levels, (2) simulate 3D microenvironment using hydrogel scaffolds, (3) incorporate human cells and control the distribution of small molecules, (4) reduce the volume of required reagents, and (5) avoid the use of expensive of ethical controversial animal models.[8,9] Over the last two decades, some reports have developed microchip compartmentalization using hydrophobicity or 3D bioprinting.[10–14] These works describe using in vitro perfusable vessels with hydrogel endothelization to mimic endothelial cell migration, vascular barrier function, and inflammatory response.[10–12] Other works have used this technology to support the study of ion transport[13] or long-term cultures of intestinal bacteria.[14] These microfluidic-based platforms were pioneers in co-culturing within confined compartments to simulate physiological conditions including molecular transport, nutrient absorption, and attempting to mimic natural endothelial morphogenesis.[10–13] Another strategy included the use of a temporary membrane to separate the parenchymal and endothelial channels.[15] But this technique presented a higher risk of channel occlusion by polymer residues. Still, these studies do not attempt to feature the dynamic and tunable properties of the native tissue microenvironment.

The current microchip design also aims to mimic the selective barrier function of blood vessels by using microfluidic technology, in 2D models, to support a capillary line pinning technique for cell compartmentalization and controllable patterning of hydrogels within the microchips: channels for the confinement of HUVECs in the lumen region; channels patterned with magnetic-responsive gelatin (mGelatin) for MSC encapsulation. The combination of MSCs and HUVECs in vascularization models was previously described to induce an increased sprouting effect, with MSCs playing a key role in secreting growth factors (e.g. VEGF) to promote HUVECs maturation.[16–20]

As mentioned before, another challenge in this area is the combination of geometric compliance with adequate biochemical stimulation (e.g., growth factors supply) to mimic the vascular microenvironment. Recent studies from the same authors showed the potential of using magnetic stimulation for local modulation of tissue vascularization, through both regulation of MSCs angiogenic behavior, through the control of biomolecules' interaction/sorption to/in magnetic-responsive hydrogels[21] and the enhanced secretion of vascular growth factors (e.g., VEGF-A).[22,23] As a key novelty strategy of this study, magnetic stimulation was here used to boost the formation of microvessel networks in 2D and 3D micro-platforms patterned with a biocompatible and magnetic-responsive hydrogel (mGelatin). When paired with a magnetic field, the magnetic hydrogel possesses unique tunable features, demonstrated by the wettability switch into a super hydrophilic surface (contact angle decreases ≈20 degrees).[22] Additionally, the hydrogel allows to mimic the elastic mechanical properties of the blood vessel tissue and supports the growth of MSC and HUVEC co-cultures while also mediating the access of cells to the magnetic stimuli produced by a neodymium bar.

In this work, three different 2D chip geometries were designed and evaluated considering their flow dynamic characteristics and their impact on cell culture behavior and angiogenesis development. Despite the capacity of 2D in vitro models to investigate vascular network-related phenomena, 3D models still offer the possibility to better mimic physiological cell-cell and cell-matrix interactions within supporting matrices.[24] For this reason, the performance of 2D geometries using microchips with capillary barriers was compared in terms of angiogenic response with 3D macroscale models of single blood vessel constructs using 3D molding techniques.

Ultimately, this study features novel magnetic-responsive platforms providing reliable and more versatile in vitro vascular models, allowing for improved HUVEC vasculogenesis, offering the possibility of cell studies under magnetic modulated angiogenic conditions, and promoting enhanced control of vascularization parameters (e.g., concentration gradients). In this regard, these magnetic-responsive vascular models are expected to bring advanced knowledge on cell mechanisms inherent to vascular ischemic diseases, boosting the development of enhanced clinical therapeutics.

2. Results

2.1. Chips and 3D Single Channel Models for In Vitro Vascularization Studies

2.1.1. Chip Models

2D chips were fabricated to enable angiogenic development on dedicated cell culture compartments under controlled fluid flow (**Figure 1**a). Three different geometries (type I, II, and III) were fabricated and assessed concerning HUVECs microvessel formation (Figure 1b). 2D chips with angular (Type I) and linear (Types II and III) shaped channels and of different widths (Type II and III) were used to compare the effect of distinct geometries on fluid flow and cell behavior, under similar perfusion conditions.

The diffusion path of all molecules and cells coming in and out of the different compartments of the 2D chips, and the interactions between them, are schematically represented in Figure 1c.

The 2D chips here prototyped were structured in polydimethylsiloxane (PDMS), via soft lithography (Figure S1, Supporting Information). The chips contained several parallel channels for cell media injection, ensuring a suitable supply of cells nutrients. PDMS cell compartments (height: 450 μm) were separated by capillary line pinning barriers (height: 150 μm) to facilitate the success of magnetic-responsive hydrogel (mGelatin) patterning and avoid hydrogel leakage (Figure S2, Supporting Information).

Another advantage of capillary barriers is the possibility to allow for diffusion between different regions of the chip. The gelatin compartment was filled with mGelatin, here used as a cell scaffold able to support MSCs and HUVECs co-cultures. The thickness of the mGelatin layer, corresponding to the total channel height, was measured at 450 μm for all the 2D chips. The width of the gelatin compartments and the media channel was 4 mm and 1.5 mm for both type I and II chips, and 8.5 mm and 2 mm for type III chips.[12,15,25] The volumes of 2D chips compartments are resumed in Figure S2 (Supporting Information). Hydrogel patterning and cell seeding procedures are illustrated in Figure S2 (Supporting Information).

The shear stress values for the feed/ cell media channels, calculated according to Equation 1, are summarized in **Table 1**.

© 2023 Wiley-VCH GmbH

2365709x, 2023, 19, Downloaded from https://onlinelibrary.wiley.com/doi/10.1002/admt.202300617 by University Of Twente Finance Department, Wiley Online Library on [21/05/2024]. See the Terms and Conditions (https://onlinelibrary.wiley.com/terms-and-conditions) on Wiley Online Library for rules of use; OA articles are governed by the applicable Creative Commons License

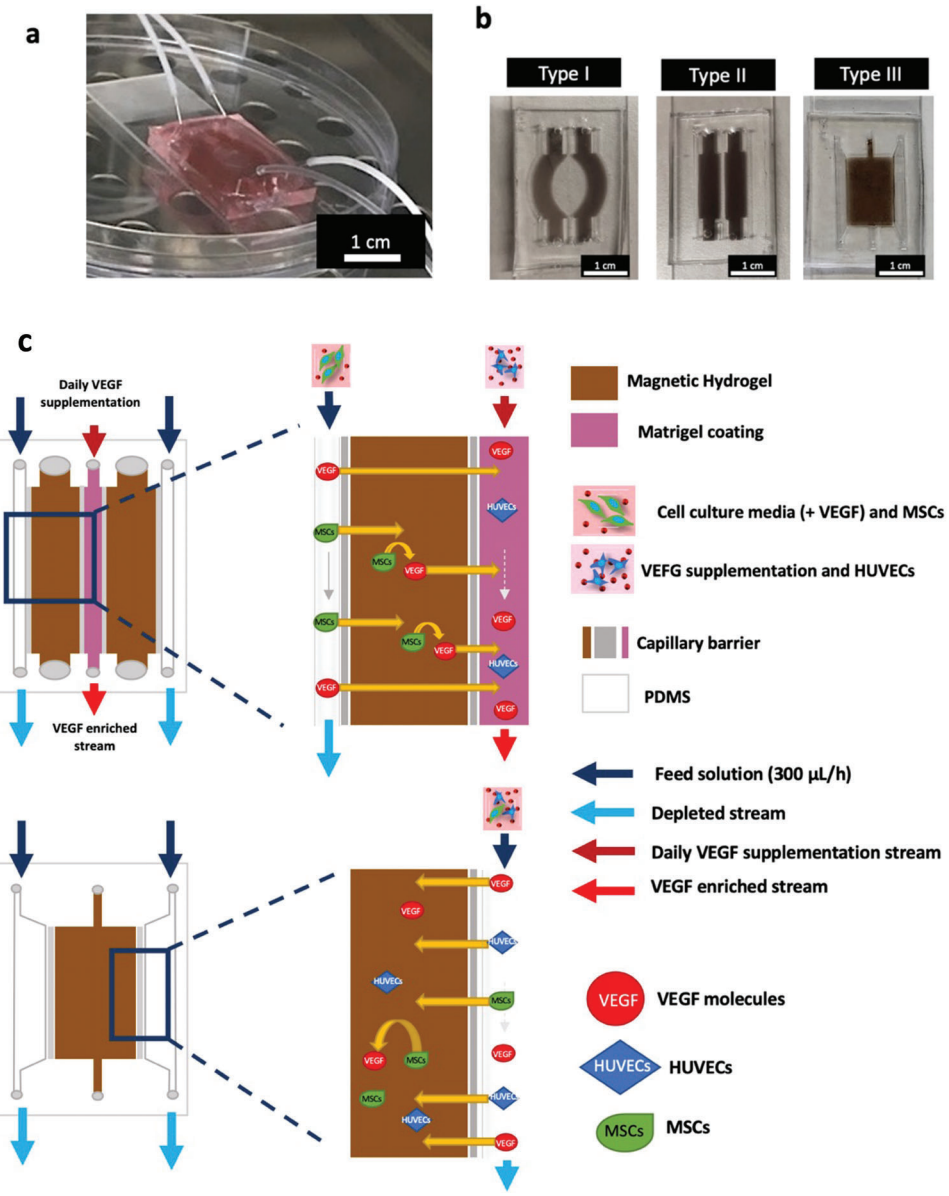

Figure 1. a) Perfusable assembled device for cellular experiments. b) 2D chips in all three geometries, with patterned hydrogels (magnetic-responsive gelatin-mGelatin). c) 2D chip types II and III with patterned hydrogels (mGelatin and Matrigel) and co-culture (MSCs and HUVECs). The scheme represents the mechanisms of cell seeding in the initial stage of the experiment and the process of VEGF transport into the HUVECs compartment. 2D chip type I has a similar mechanism to type II.

Table 1. Determination of wall shear stress in the 2D chip types.

	Symbol	Type I	Type II	Type III	*Si unit*
Dynamic viscosity	μ	1100	1100	1100	Ns m^{-2}
Volumetric flow rate	Q	8.34×10^{-11}	8.34×10^{-11}	8.34×10^{-11}	m^3 s^{-1}
Width of the media channel	W	1.5×10^{-3}	1.5×10^{-3}	2×10^{-3}	m
Height of the channel	H	0.45×10^{-3}	0.45×10^{-3}	0.45×10^{-3}	m
Wall Shear Stress	τ_W	1.81×10^{3}	1.81×10^{3}	1.36×10^{3}	N m^{-2}

© 2023 Wiley-VCH GmbH

2365709x, 2023, 19, Downloaded from https://onlinelibrary.wiley.com/doi/10.1002/admt.202300617 by University Of Twente Finance Department, Wiley Online Library on [21/05/2024]. See the Terms and Conditions (https://onlinelibrary.wiley.com/terms-and-conditions) on Wiley Online Library for rules of use; OA articles are governed by the applicable Creative Commons License

$$\tau = (6\mu Q) / (WH^2) \quad (1)$$

where μ is the fluid viscosity, Q is the flow rate, and W and H are the width and height of the microfluidic channel, respectively.

Low shear stress values were obtained in the 2D chips, corresponding to laminar fluid conditions, known to be crucial for normal vascular functioning, including regulation of vascular caliber, inhibition of proliferation, thrombosis, and inflammation of the vessel walls.[26] Regardless of the different widths of the media channels, larger for type III chips, no significant changes in the shear stress were estimated between the 2D chip types.

MSCs and HUVECs were seeded through the media channels. MSCs were expected to migrate from the cell media channel to the mGelatin matrix (gelatin compartment), whereas HUVECs were expected to adhere to the Matrigel coating in the central compartment of the chips, as illustrated in Figure S3 (Supporting Information). MSCs were used as a source of pro-angiogenic factors, such as VEGF, for prompting the angiogenesis of HUVECs, with the formation of an artificial microvasculature.

2.1.2. 3D Single Channel Models

The 2D microfluidic chip geometries were compared to single-channel 3D constructs fabricated through molding techniques to mimic the dimensions of larger arteries and veins with an outer diameter of 2 cm (**Figure 2**a). The vein model comprised a larger inner diameter of 1.8 cm than the artery model with a 0.3 cm inner diameter, corresponding to 0.2 and 1.7 cm wall thicknesses for the vein and the artery models, respectively. These geometries allow for mimicking the larger arteries' anatomic wall thickness. Despite the inexistence of capillary barriers in these 3D models, MSCs were cultured on the outer wall and HUVECs were seeded on the lumen of the models to mimic biology (Figure 2b). Mechanical testing of the mGelatin was performed to compare the elasticity of the anatomic 3D model, composed of elastin fibers (0.5 MPa[27]), smooth muscle (0.01 MPa[28]), and collagen fibers (500 MPa[27]) (Figure 2c). Stress-strain curves plotting loading forces (MPa) with deformation (mm) were traced for each sample and the Young Modulus was calculated for the mGelatin before and after crosslinking (0.26 ± 0.03 MPa and 2.31 ± 0.11 MPa, respectively). The elasticity modulus of crosslinked mGelatin was higher than for elastin fibers and smooth muscle but lower than collagen fibers, suggesting it remains within the biological featuring dimensions.

2.1.3. VEGF Molecule Concentration and Velocity Profile Simulations in 2D Chips

A major aspect to promote microvascular formation within the 2D chips relates to the concentration gradients and the availability of pro-angiogenic factors, such as VEGF.

Computational studies were performed to study the impact of the different 2D configurations on the access of HUVECs to VEGF molecules. COMSOL Multiphysics software was used to predict the diffusion and the linear velocity profiles of VEGF within the chip compartments, allowing to optimize the supply of this key molecule to the HUVECs compartment and, therefore, the maturation and vasculogenesis of these cells. All assumptions used in the COMSOL simulation are described in Section S4 (Supporting Information). The different 2D chips, patterned with mGelatin, were compared in terms of VEGF concentration outlets for 1 µg mL^{-1} of VEGF solution. The simulation of VEGF transport within the channels showed that VEGF molecules were able to diffuse through the compartments in every 2D chip type despite diffusional limitations imposed by the gelatin barrier. A slower diffusion of VEFG was estimated for chips type I and II (**Figure 3**a), possibly due to a higher accumulation of VEGF in the feed compartment of 2D chip type III, which has a larger cross-section channel. However, it is important to highlight that these mathematical models take into account the chips' geometric features and inlet fluid conditions, but not the presence of the cells and their metabolism.

These results are in good agreement with experimental observation, assessed by experimental quantification of VEGF-A at the outlet streams, showing values of 4000 pg mL^{-1}, 3500 pg mL^{-1}, and 5000 pg mL^{-1}, respectively, for chips type I, II, and III, at the end of the experiment (day 7) (Figure 3b). The quantification of VEGF in chips types I and II was performed in the fluid after VEGF gelatin permeation, while for type III chips it was assessed in the media channel outlet. Therefore, the lower VEGF outlet concentration found for chip types I and II may be associated with higher retention of VEGF in the gelatin matrix (by adsorption to the matrix or imprisonment in the pores of the gelatin hydrogel).

The linear velocity profiles of VEGF in the media channels were also predicted by COMSOL showing similarities in the performances of type I and II while indicating a slower velocity profile on type III (**Figure 4**a), which can be attributed to the larger feed flow channel width of type III chip.

Fluorescent tracers were added in the perfusing media of 2D chip flow channels (Figure 4b) for validation of the simulated linear profiles (see Section S4, Supporting Information), resulting in experimentally estimate average velocities of 6.7×10^{-7}, 5.5×10^{-7}, and 2.0×10^{-7} m s^{-1} for chips type I, II, and III, respectively. Such values are in good agreement with the ones obtained by the computational simulation, with 6.2×10^{-7}, 5.8×10^{-7}, and 1.8×10^{-7} m s^{-1} for types I, II, and III, respectively.

2.2. Endothelial Culture Strategies for 2D and 3D Models

HUVEC culture conditions were studied and optimized to prompt angiogenic behavior. The initial studies were performed using HUVECs monocultures, thus excluding the endogenous VEGF produced by MSCs, and relying on the VEGF content in cell media (1 µg mL^{-1}) as the only pro-angiogenic factors source. Angiogenic behavior was assessed considering HUVECs' adherence to channel walls, proliferation, migration within the channel lumen or walls, and the formation of endothelial tissue with the development of tube-like forms (Table S1, Supporting Information).

The impact of media feeding strategies on HUVECs behavior, in 2D models, was first assessed, considering: 1) single daily renewal of the media (static feeding condition), and 2) continuous media perfusion, applied with a syringe pump (Harvard

© 2023 Wiley-VCH GmbH

2365709x, 2023, 19, Downloaded from https://onlinelibrary.wiley.com/doi/10.1002/admt.202300617 by University Of Twente Finance Department, Wiley Online Library on [21/05/2024]. See the Terms and Conditions (https://onlinelibrary.wiley.com/terms-and-conditions) on Wiley Online Library for rules of use; OA articles are governed by the applicable Creative Commons License

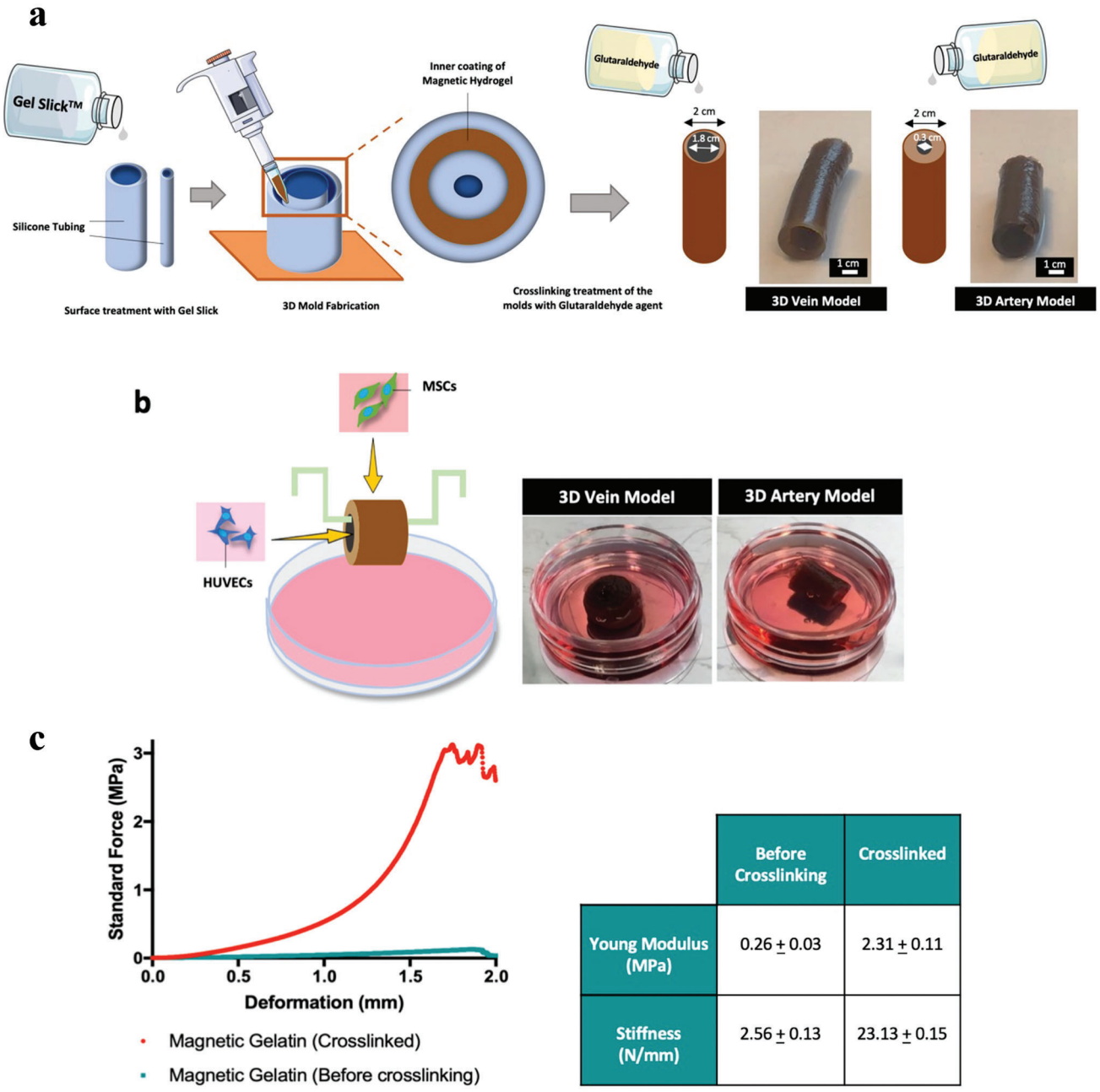

	Before Crosslinking	Crosslinked
Young Modulus (MPa)	0.26 ± 0.03	2.31 ± 0.11
Stiffness (N/mm)	2.56 ± 0.13	23.13 ± 0.15

Figure 2. a) Molding fabrication procedures for the 3D single channel model of magnetic gelatin. b) Schematic representation of the cell culture seeding on the 3D models. c) Representative stress-strain curves for the mechanical characterization by compression testing of the magnetic gelatin (arteries and vein model materials) before and after crosslinking with glutaraldehyde. Corresponding Young´s Modulus values are indicated in the table (inset).

Apparatus, PHD2000) at a flow rate of 300 µL h^{-1}, promoting constantly media renewing.

Phase contrast images showed that both static and perfusion methods allowed for HUVECs adherence to the channel walls at day 2 (two days following HUVECs seeding). However, the perfusion mode promoted faster cells migration from the HUVECs compartment to the gelatin compartment, as HUVECs were visualized in the gelatin after day 4, whereas in static mode, only at day 7 cells were observed at the gelatin wall (**Figure 5**a). The area of cell migration at the gelatin wall was quantified using ImageJ. While on day 2 no significant area was found for either perfusion or static mode, differences were found from day 4, with a measured area of cell migration of 4189.4 μm^2, under perfusion, and only 1285.2 μm^2, under static mode. At day 7, the cell migration area was of 13176.4 μm^2 for perfusion mode and 7214.7 μm^2 for static configuration, thus confirming a faster migration, for the same period, under perfusion mode. This mobility is compatible with HUVECs behavior in a pre-angiogenesis stage, before their remodeling into tubular structures, and is known to be regulated by VEGF concentration gradients.[29] Therefore, the movement

© 2023 Wiley-VCH GmbH

2365709x, 2023, 19, Downloaded from https://onlinelibrary.wiley.com/doi/10.1002/admt.202300617 by University Of Twente Finance Department, Wiley Online Library on [21/05/2024]. See the Terms and Conditions (https://onlinelibrary.wiley.com/terms-and-conditions) on Wiley Online Library for rules of use; OA articles are governed by the applicable Creative Commons License

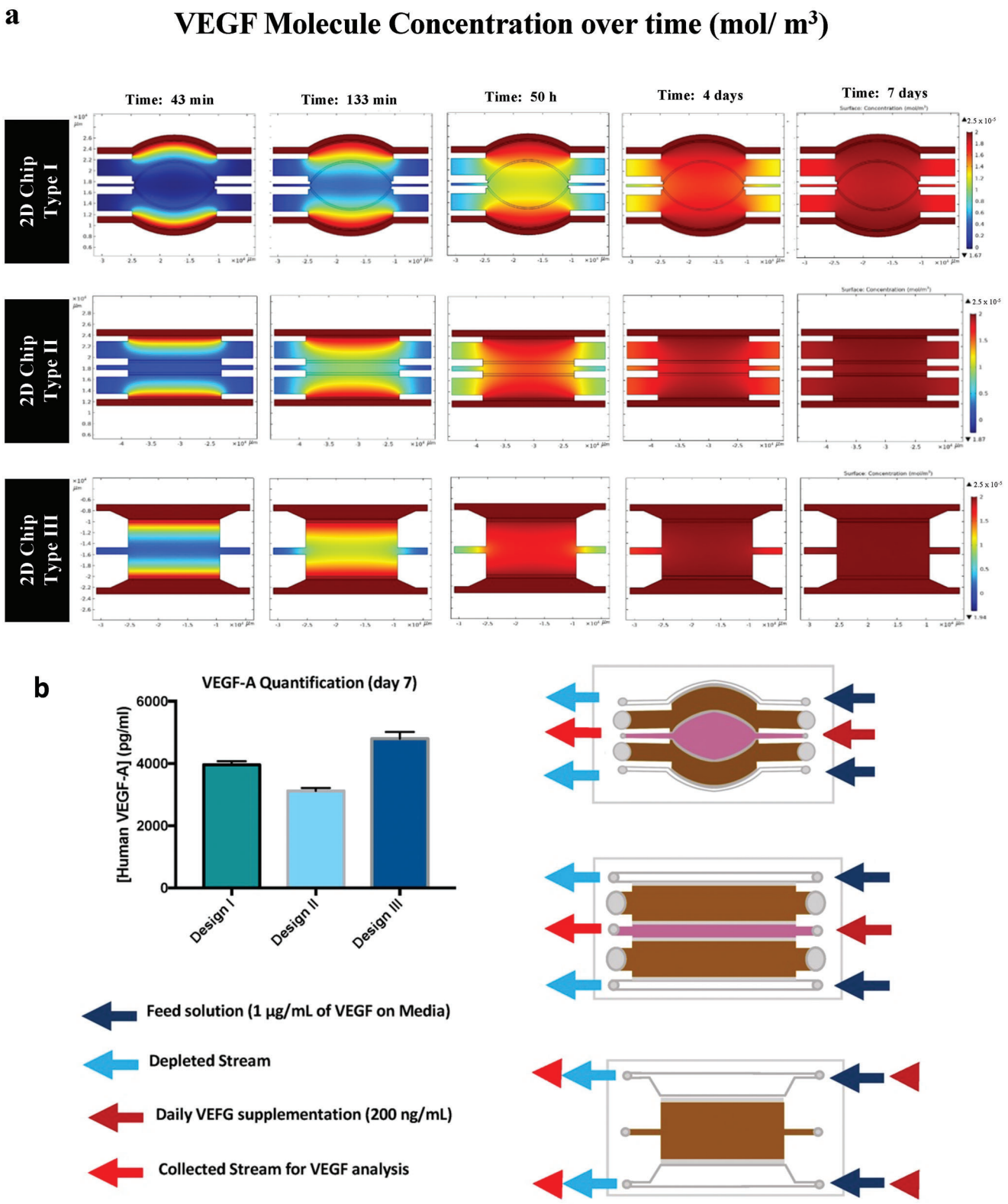

Figure 3. a) COMSOL simulation results for the VEGF time-dependent concentration from the media channels to the endothelial cell (HUVECs) culture compartment in 2D chip models. The sequential images of the VEGF diffusion are presented as contour plots of the surface concentration of VEGF inside the chips. b) VEGF concentration in the outlet streams of 2D chips was quantified by ELISA for experimental validation of the diffusion models.

© 2023 Wiley-VCH GmbH

2365709x, 2023, 19, Downloaded from https://onlinelibrary.wiley.com/doi/10.1002/admt.202300617 by University Of Twente Finance Department, Wiley Online Library on [21/05/2024]. See the Terms and Conditions (https://onlinelibrary.wiley.com/terms-and-conditions) on Wiley Online Library for rules of use; OA articles are governed by the applicable Creative Commons License

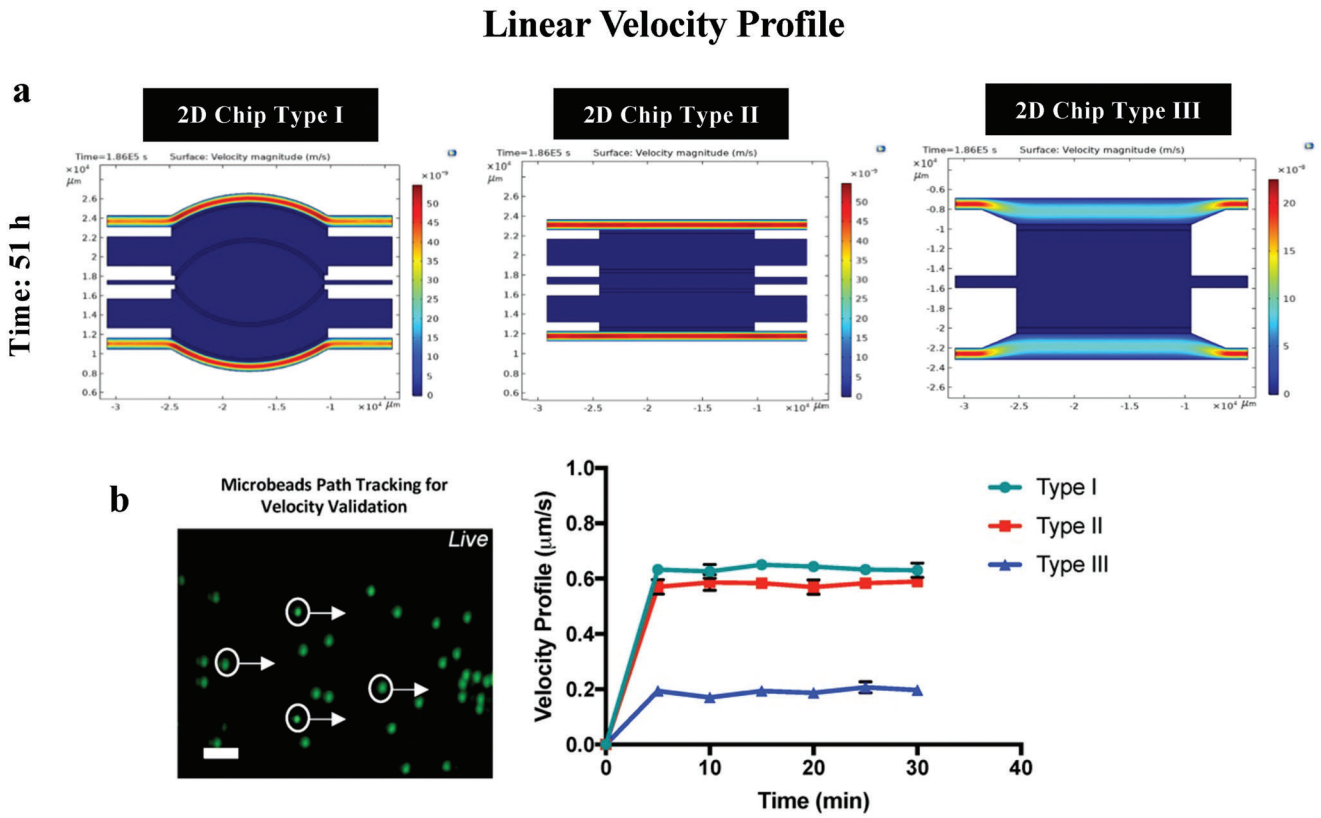

Figure 4. a) Linear velocities distribution within the 2D chip media channels calculated by computational fluid flow modeling. b) Validation of the prediction model using fluorescent microbeads (15 μm) to trace the velocity profiles for the 2D chips with an experimental flow velocity of 300 μL h^{-1}. Microbeads tracking velocity was obtained using ImageJ software. Tracking analysis was performed on three points of the channel for each design. Scale bar: 100 μm.

of HUVECs toward the borderline of the gelatin channel may be explained by the VEGF concentration build-up at the gelatin wall and the consequential increase of the VEGF concentration gradient between the cell media bulk (flowing in the media channels) and the gelatin compartment.

HUVECs adhesion, although at a lower extent than for 2D chips, was also observed in 3D models. No differences in HUVECs migration between static or perfusion modes were registered (Table S1, Supporting Information). The adherence and proliferation of HUVECs over time were also investigated by calcein assay for cell viability analysis at days 1, 4, and 7 (Figure 5b) for 3D models and 2D chips type II. A small population of HUVECs was found attached to the gelatin walls of all the chips, at day 1. 2D chip type I and II showed similar performances, but endothelialization was not observed in type III chips (Table S1, Supporting Information).

After 7 days, HUVECs were able to establish a ramified monolayer on the representative 2D chip type II, but not on the 3D chips. Indeed, for the 3D models, despite HUVECs proliferation and their adherence to the walls at days 4 and 7, these cells still appeared individualized and without signs of sprouting structures at day 7 (Figure 5b; Table S1, Supporting Information). The 3D artery model showed even poorer HUVECs adhesion in the gelatin walls and displayed fewer cells on the inner surface, in comparison with the 3D vein model (Figure 5b).

Optimization experiments, using different concentrations of MSCs and HUVECs, were performed through a preliminary co-culture trial. Initial lower concentration of MSCs (5×10^4 cells mL^{-1}) and HUVECs (1.5×10^5 cells mL^{-1}) resulted in poor outcomes regarding adhesion, migration, and sprouting, whereas a significantly better adhesion was found at higher cell concentrations of 1.5×10^6 cells mL^{-1} for MSCs and 3×10^6 cells mL^{-1} for HUVECs (Table S1, Supporting Information). At this stage, the goal was to obtain indications of early angiogenesis through observation of sprouting and migration in HUVECs and the initial development of an interconnected monolayer. This monolayer will be stimulated to further grow and endothelialize the channels in the presence of a magnetic field in later experiments.

Despite the cell migration and adhesion, these preliminary results showed the need for additional strategies to stimulate vasculogenesis since the formation of an interconnected matrix (endothelization) was not observed in normal culture conditions.

Consequently, on further co-cultures (Figure S5, Supporting Information), VEGF was daily supplemented (0.2 μg mL^{-1}) directly on the cell culture compartment, increasing this molecule gradient in the HUVECs compartment, hence stimulating the maturation of the cells into the endothelial matrix (Table S1, Supporting Information). This strategy resulted in improved angiogenic results for 2D chips type I and II, with endothelialized

© 2023 Wiley-VCH GmbH

2365709x, 2023, 19, Downloaded from https://onlinelibrary.wiley.com/doi/10.1002/admt.202300617 by University Of Twente Finance Department, Wiley Online Library on [21/05/2024]. See the Terms and Conditions (https://onlinelibrary.wiley.com/terms-and-conditions) on Wiley Online Library for rules of use; OA articles are governed by the applicable Creative Commons License

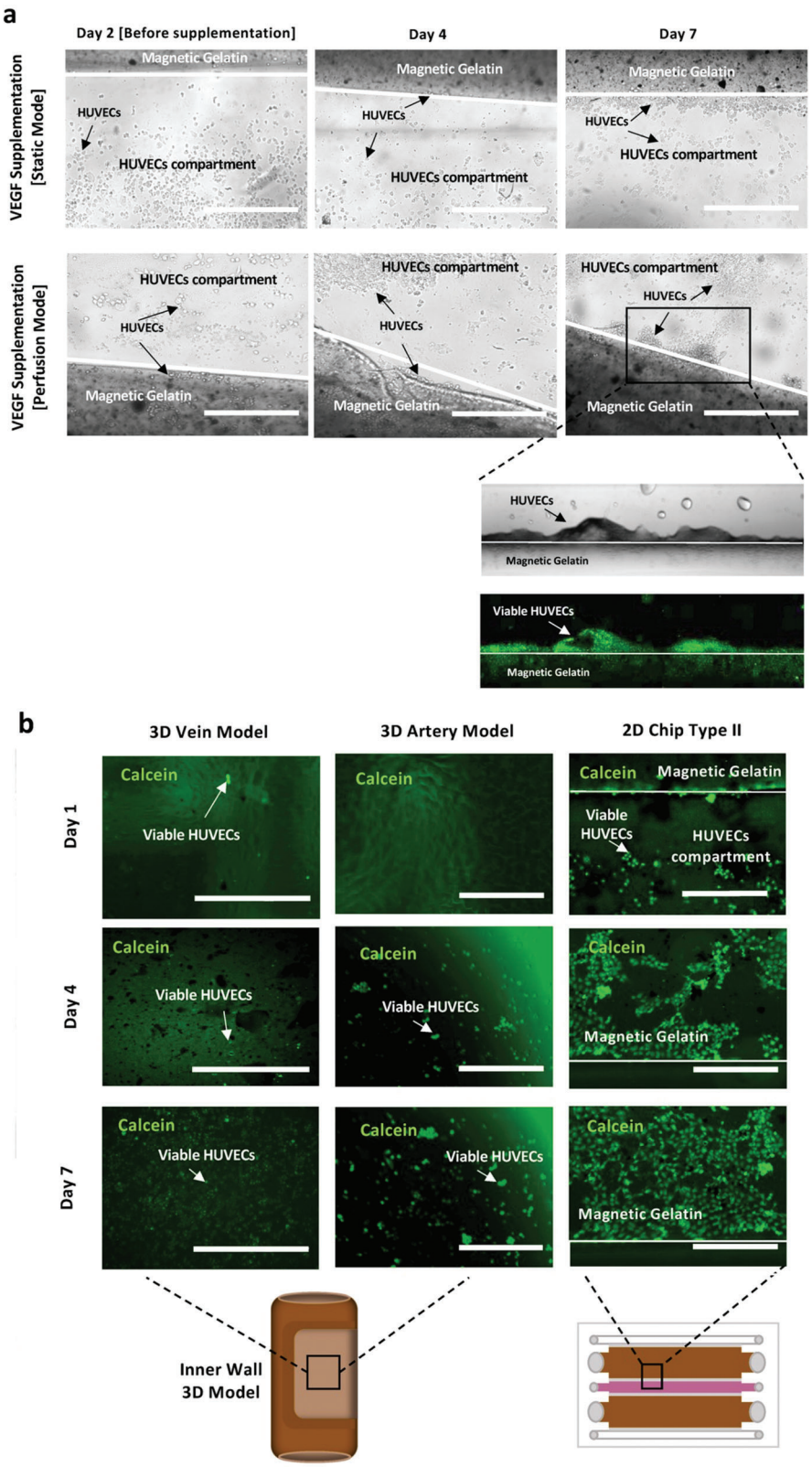

Figure 5. a) Top view phase contrast images of HUVECs migration overtime before VEGF supplementation (day2) and after supplementation (day 4 and 7) depending on the feeding mode (static or perfusion) on 2D chips type I. Scalebar: 1000 µm. b) Fluorescence imaging of viable HUVECs to assess adherence and proliferation (days 1, 4, 7) under perfusion mode for 2D chip type II and 3D vein and artery models. Scalebar: 1000 µm.

© 2023 Wiley-VCH GmbH

2365709x, 2023, 19, Downloaded from https://onlinelibrary.wiley.com/doi/10.1002/admt.202300617 by University Of Twente Finance Department, Wiley Online Library on [21/05/2024]. See the Terms and Conditions (https://onlinelibrary.wiley.com/terms-and-conditions) on Wiley Online Library for rules of use; OA articles are governed by the applicable Creative Commons License

matrix being observed in some regions of the chips, after day 4 (Figure S5, Supporting Information). However, upon additional VEGF supplementation, the formation of an endothelial monolayer was not observed in 2D chip type III, possibly due to transport limitations of nutrients and VEGF to the cells compartment. In the type III chip, the HUVECs are entrapped into the mGelatin matrix, in contrast to types I and II, where HUVECs are located in a thin Matrigel coating at the surface of the mGelatin compartment. In 3D models, no improvement regarding endothelialization of the cells was observed from VEGF supplementation (Table S1, Supporting Information).

Although VEGF supplementation revealed improvements (in Type I and II), this strategy alone was not efficient in triggering an angiogenic behavior on HUVECs. Therefore, a second strategy was implemented, consisting of daily adding HUVECs to the system, at a lower concentration (3×10^4 cells mL^{-1}), in the HUVECs compartment in 2D chips and the lumen of 3D models. This strategy led to the successful formation of a ramified matrix in 2D types I and II. Finally, the VEGF supplementation and multiple cell seeding strategies were combined, boosting HUVECs' performance, ensuring the formation of a microvascular monolayer on the channels of chips I and II (Table S1, Supporting Information) and resulting in a successful proangiogenic effect with the formation of tube-like structures (**Figure 6**a).

To observe the tube-like structures and branch points, three stainings were performed in Figure 6a: DAPI (4′,6-diamidino-2-phenylindole - a blue cell nuclei marker for HUVECs and MSCs), YoYo (one of the highest affinity nucleic acid stains, it shows over a thousand-fold increase in its green fluorescence when bound to dsDNA) and Ethidium homodimer I solution - EthD (used to stain red the nuclei of dead or apoptotic cells, showing morphological differences between late apoptotic cells and necrotic cells with fragmented nuclei). The fixed cells in Figure 6a do not show signs of necrosis, instead allowing us to clearly observe interconnected cells, a sign of HUVECs´ viability and angiogenic behavior.

The endothelization was observed only in small regions of 3D models, confirming that the supplementation strategies were not as efficient in 3D models as in 2D chips type I and II, where the feeding process was more controlled. No endothelization was observed using type III (Table S1, Supporting Information), which was probably associated with the limiting access of HUVECs to the growth factors, i.e. VEGF, as explained previously.

A Layer-by-Layer (LbL) construct, featuring two mirrored layers of the same geometry (type I, II, or III) bonded together after microscopic alignment (Figure 6b), was fabricated to maximize the circulating volume of cell culture medium within the chips (twice the volume of regular chip types) and assessed for potential improvement in the endothelization process. The strategy of combining VEGF supplementation and HUVECs multiple seeding was evaluated using the LBL and the original chip configurations (Figure 6b).

The sprouting parameters were quantified by analyzing three regions from independent experiments and by measuring the number and length of tubes formed using ImageJ software (95% of confidence level), for original 2D chips type I and II (no tubes were observed on 2D chip type III) and the respective LbL structures. LbL configurations showed improved results, leading to the formation of ca. 98 microtubes, in contrast with 59 average tubes quantified with original chips (Type I and II) (Figure 6b). It was concluded that the LBL type I and type II chips promoted cell proliferation, migration behavior (cells migrated from their compartment to the gelatin compartment), and progressive formation of microvascular monolayer, after 7 days. The same promising results involving the formation of a microvessel layer were also observed on the LbL type III chip, which had not been accomplished using the original type III configuration (Figure 6b). The increase in the angiogenic behavior of HUVECs was possibly due to the duplicate increase of cell medium volume and increased surface area, allowing a higher concentration of oxygen, nutrients, and growth factors to the same concentration of cells and diffusion distance as the original type III.

2.3. Co-Culture of MSCs and HUVECs With Magnetic Stimulation

MSCs and HUVECs co-culture was performed, as a proof of concept, using the best performing 2D chips type I and II, and 3D vein model at the conditions that promoted endothelization: perfusion of the cells media/feed solution over 7 days combined with both VEGF and multiple HUVECs seeding. The use of magnetic stimulation as a strategy to increase cellular stress, boost VEGF secretion from MSCs, and thus promote microvascular formation[23] was also evaluated.

Hence, a static magnetic field of 0.08 T was applied over the last 24 h of the experiment (from day 6 to day 7) and compared with models not exposed to the magnetic field. After the exposure of the models to the magnetic field, the exogenous VEGF supplementation and multiple HUVECs seeding were interrupted to clarify the effect of magnetic stimulation.

The effect of the magnetic field on the behavior of MSCs and HUVECs co-cultures in 3D models was also evaluated by comparative imaging of the lumen, the cross-section, and the outer wall obtained by confocal microscopy (**Figure 7**a). The results confirmed the cell's ability to populate the three regions of the 3D structure. However, interestingly the formation of an endothelial monolayer, representing the initial stages of endothelial tissue, was only observed in 3D vein models when exposed to the magnetic field.

The magnetic field was found to increase cell viability (Figure 7b) on 2D chips (as detected by live – green Calcein AM – and dead – EthD - markers). The effect of the magnetic field on HUVECs survival was potentially associated with the increased release of growth factors to the medium due to the magnetic stimulation of the MSCs (Figure 7b). Moreover, the formation of an interconnected endothelial monolayer was only observed in the chips stimulated at 0.08 T and absent on chips not exposed to the magnetic field (Figure 7c). Similar results were obtained for 2D chip types I and II, in terms of the effect of the magnetic field on the cells, therefore representative images of both chips are shown in Figure 7b–d.

The effect of the magnetic field on HUVECs survival (≈60% cell death in the non-exposed microchips in comparison with 5% cell death in the microchips under magnetic stimulation) was potentially associated with the increased release of growth factors to the medium in response to the magnetic stimulation of the

© 2023 Wiley-VCH GmbH

2365709x, 2023, 19, Downloaded from https://onlinelibrary.wiley.com/doi/10.1002/admt.202300617 by University Of Twente Finance Department, Wiley Online Library on [21/05/2024]. See the Terms and Conditions (https://onlinelibrary.wiley.com/terms-and-conditions) on Wiley Online Library for rules of use; OA articles are governed by the applicable Creative Commons License

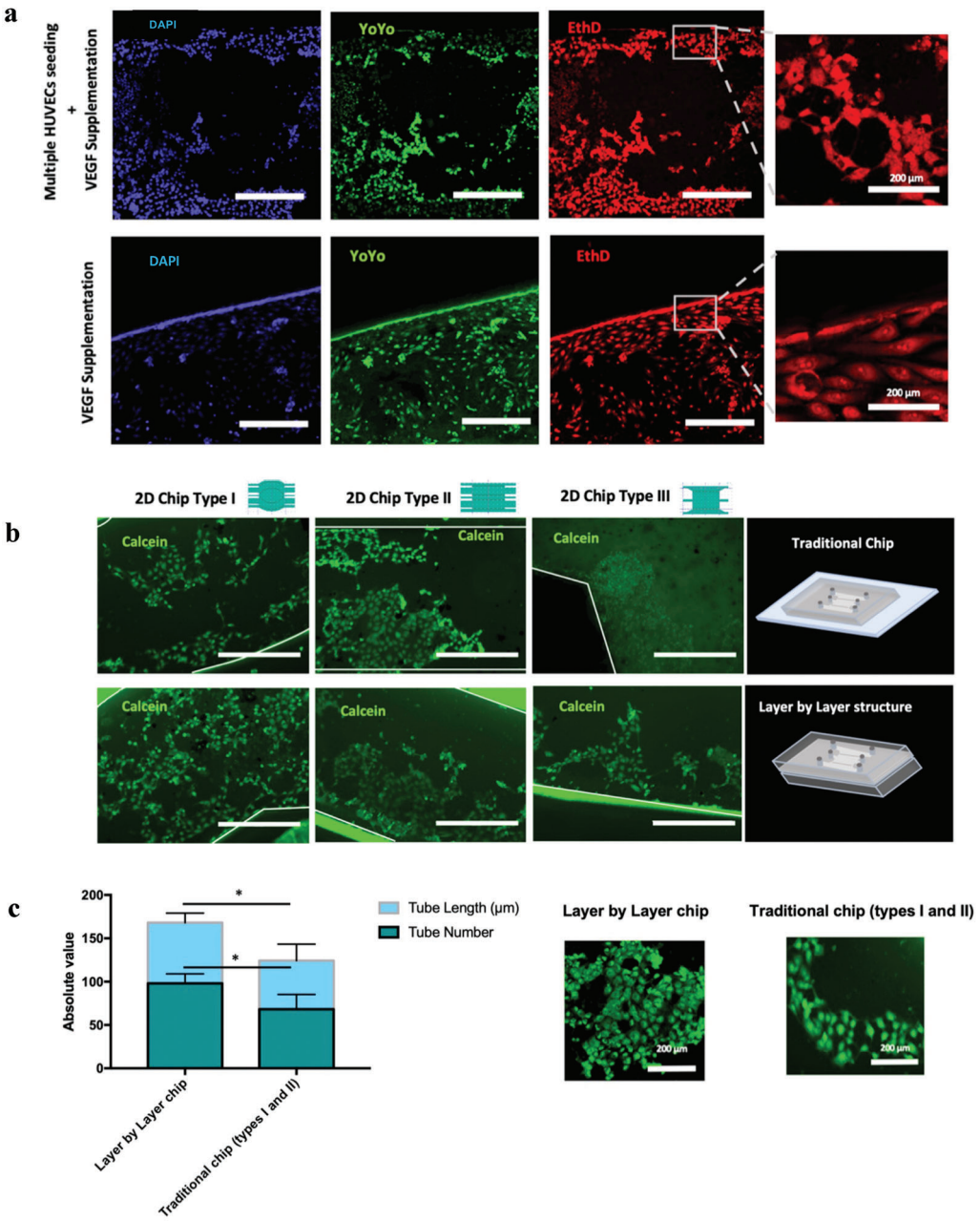

Figure 6. a) Confocal imaging (DAPI, YoYo, EthD) of endothelial tissue and sprout ramifications for 2D chips Type II (7 days, perfusion mode) using VEGF supplementation strategy. Comparison with the strategy combining VEGF supplementation and multiple HUVECs seeding. Scalebar: 1000 µm. b) Characterization of viable HUVECs proliferation and tissue formation after 7 days using traditional one-layer configuration and layer-by-layer chip (for all three types) under perfusion, VEGF supplementation and HUVECs multiple seeding conditions. Scalebar: 1000 µm. c) Quantification of tube number and tube length, for each configuration. Statistical significance was determined using two-Way ANOVA. Data presented as means ± SD.

MSCs (Figure 7b). These results are in total agreement with the proangiogenic effect of the magnetic field described in previous publications by this group.[23,24] The magnetic field has been shown to enhance the angiogenic potential of MSCs through the secretion of VEGF, thus promoting tube formation in HUVECs when they are cultured in a conditioned medium from MSCs (enriched in VEGF[16]). The cell death observed in 2D chips not exposed to the magnetic field (Figure 7b) might be attributed to MSCs-HUVECs contact inhibitions. Despite the initial seeding of the cells in different compartments, it may be hypothesized that the contact between MSCs and HUVECs possibly originated from cell migration between channels, which was confirmed through Live/Dead tests (Figure 7b).

Immunostaining using CD31 (HUVEC-specific antibody) and DAPI was also performed to distinguish HUVECs and MSCs colonies on 2D chips (Figure 7d), revealing that while the

© 2023 Wiley-VCH GmbH

2365709x, 2023, 19, Downloaded from https://onlinelibrary.wiley.com/doi/10.1002/admt.202300617 by University Of Twente Finance Department, Wiley Online Library on [21/05/2024]. See the Terms and Conditions (https://onlinelibrary.wiley.com/terms-and-conditions) on Wiley Online Library for rules of use; OA articles are governed by the applicable Creative Commons License

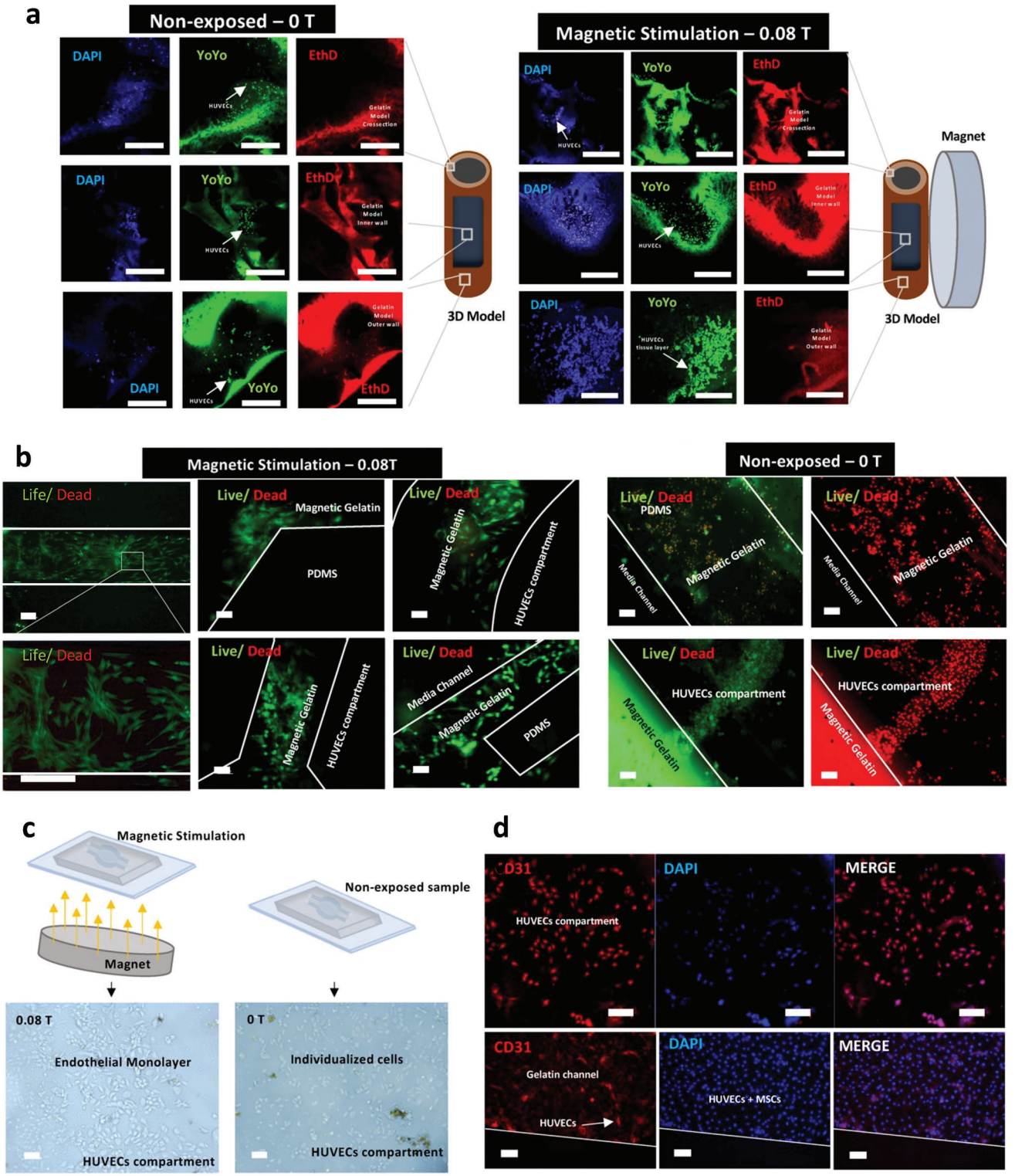

Figure 7. a) Confocal imaging (DAPI, YoYo, and EthD) of MSCs and HUVECs co-culture (day 7) on representative 3D models (Vein). A magnetic field (0.08 T) was applied on day 6 for a total exposure of 24 h and directly compared with non-exposed samples (control) Scalebar: 1000 µm. b) Live and dead (Calcein and EthD) representative images of 2D chips (Type I) showing a co-culture of MSCs and HUVECs exposed to magnetic stimulation (0.08 T) at day 7 compared with chips not exposed to magnetic stimulation. Scalebar: 100 µm. c) Phase contrast images evidencing endothelialization on HUVECs compartment (2D chip type I) from day 7 in comparison with the control condition. Scale bar: 100 µm. d) Immunofluorescence images (CD31 and DAPI) of the co-culture allow to distinguish between the population of HUVECs and MSCs, at day 7. Scalebar: 100 µm.

© 2023 Wiley-VCH GmbH

2365709x, 2023, 19, Downloaded from https://onlinelibrary.wiley.com/doi/10.1002/admt.202300617 by University Of Twente Finance Department, Wiley Online Library on [21/05/2024]. See the Terms and Conditions (https://onlinelibrary.wiley.com/terms-and-conditions) on Wiley Online Library for rules of use; OA articles are governed by the applicable Creative Commons License

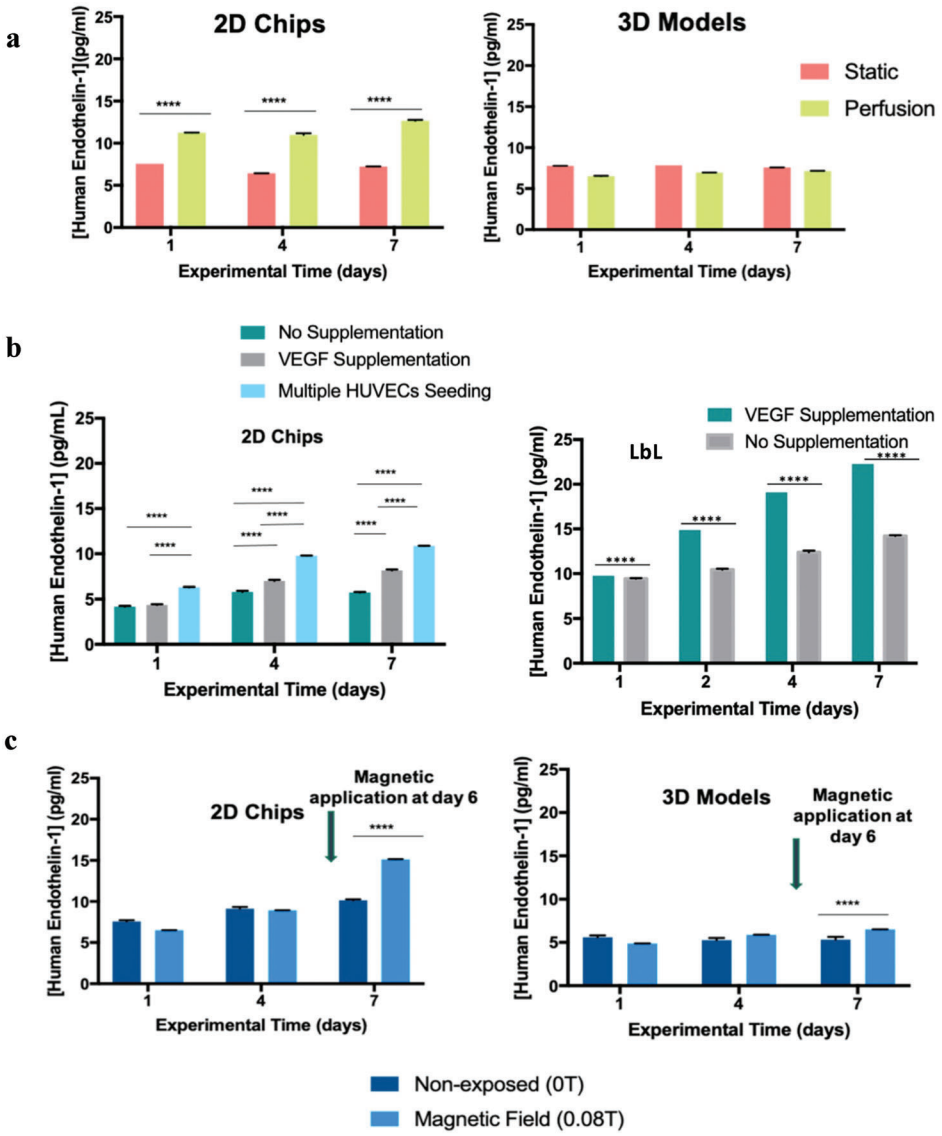

Figure 8. a) Quantification of Endothelin-1 on 2D chips (mean value for type I and II) and 3D models (artery and vein) comparing the effects of static and perfusion mode on the stimulation of endothelium tissue formation. No magnetic field was applied in this comparison. b) Impact of the different tested strategies (multiple HUVECs seeding to boost sprouting or VEGF daily supplementation) under perfusion on the increase of Endothelin-1 concentration. Comparison between 2D chips and LbL models for the conditions: VEGF supplementation and no supplementation. No magnetic field was applied on these conditions. c) Representation of the concentration of Endothelin-1 molecule derived from magnetic stimulation applied on the last day of the experiment on 2D Chips (mean value for type I and II) and 3D models (mean value) using perfusion mode. Non-exposed samples were used as a control (0 T). No VEGF supplementation was performed during magnetic application. Statistical significance was determined using two-Way ANOVA. Data presented as means ± SD.

HUVECs compartment was populated mostly by HUVECs (DAPI+, CD31+), the gelatin channel presented approximately 15% of HUVECs (DAPI+, CD31+) mixed with MSCs (DAPI+, CD31-). Additional images of CD31 staining of HUVECs in a co-culture of HUVECs and MSCs can be found in Figure S6 (Supporting Information). This observation confirmed the high motility of the HUVECs between the compartments while illustrating the efficiency of the capillary barriers to confine MSCs in the gelatin compartment. This effect was observed in the presence and absence of a magnetic field, but cell death was only visible in the latter condition, confirming the positive impact of the magnetic field on cell survival in addition to the stimulation of the endothelialization processes.

2.4. Endothelin-1 Secretion by HUVECs on 2D and 3D Models

Endothelin-1 is a vasoconstrictor secreted by endothelial cells and regulated by physical factors, e.g. shear stress, or growth factors concentration.[30] As a main regulator of the vascular function and endothelium marker, the presence of endothelin-1 in the 2D (results for type I and II) and 3D models (results for artery

© 2023 Wiley-VCH GmbH

2365709x, 2023, 19, Downloaded from https://onlinelibrary.wiley.com/doi/10.1002/admt.202300617 by University Of Twente Finance Department, Wiley Online Library on [21/05/2024]. See the Terms and Conditions (https://onlinelibrary.wiley.com/terms-and-conditions) on Wiley Online Library for rules of use; OA articles are governed by the applicable Creative Commons License

and vein models) was quantified by using Endothelin-1 ELISA (**Figure 8**), for the conditions previously assessed, to confirm the formation of premature endothelium and evaluate the effect of the different strategies to promote angiogenesis.

The results showed a significant increase in the Endothelin-1 concentration in 2D chips operated in perfusion mode in comparison to static conditions, while the secretion of endothelin-1 in 3D models did not present significant changes with the flow regime (Figure 8a). Endothelin-1 secretion increased after VEGF supplementation and HUVECs daily seeding in 2D chips (Figure 8b). The most prominent result, however, was observed with the LbL 2D chips, with Endothelin-1 secretion higher than all other conditions. This increment was further increased upon the combination with VEGF supplementation, highly boosting the secreting of this vascular regulator molecule (Figure 8b).

Finally, magnetic stimulation (0.08 T) was applied to the models over the last 24h of the experiment (at day 6), following previous angiogenic studies using short-term magnetic stimulation.[23] A positive magnetic effect was demonstrated in both 2D and 3D models, through an increased concentration of Endothelin-1 in the medium (Figure 8c) particularly noticeable in 2D chips. The concentration of endothelin-1 upon magnetic stimulation exceeded the values achieved with daily VEGF supplementation or multiple HUVECs seeding, thus revealing the importance of low-intensity static magnetic exposure to trigger angiogenic mechanisms and tissue endothelization without further need to implement strategies for VEGF supplementation.

3. Discussion

This work focused on the development of novel magnetic-responsive vascular platforms (2D chips and 3D models), aiming to provide reliable in vitro models of vascular-related diseases (e.g. cardiac ischemia, tumor metastasis, or diabetic vasculopathy) by prompting vasculogenesis phenomena. These platforms intend to be used for drug screening studies while contributing to increasing the knowledge of cell mechanisms and, hence, the development of more efficient therapeutics. The 2D chips designed consisted of microfluidic platforms patterned with magnetic-responsive gelatin (mGelatin) scaffolds containing encapsulated MSCs. VEGF secretion by MSCs can be increased upon magnetic stimulation,[23] thus this system allows to modulate the vasculogenesis of HUVECs seeded in a central compartment (lumen). 3D vascular models mimicking the anatomic morphology and mechanical properties of larger arteries (0.3 cm of inner diameter and 0.85 cm wall thickness) and veins (1.8 cm of inner diameter and 0.1 cm wall thickness) were also fabricated using mGelatin as the model matrix.

The mechanical properties of arteries have been associated with aging-related diseases, including coronary heart disease and atherosclerosis, whereas morphological aspects, such as higher thickness are associated with increased stiffness of carotid arteries.[31,28]

Here, non-cytotoxic mGelatin crosslinked with glutaraldehyde[22] (Figure S7, Supporting Information) was used as a strategy to adjust the elasticity of 3D artery and vein models, rendering artificial vessels with an elastic modulus of 2.31 ± 0.11 MPa. While blood vessels have been described to possess a lower Young's Modulus between 20–200 kPa (after expansion),[31] the magnetic gelatin can be found within the elasticity range of blood vessels components, i.e. elastin and smooth muscle ranging between 0.05–0.5 MPa and collagen with ≈500 MPa[27] (Figure 2c).

The 2D chip types I and II performed successfully and better than the 2D chip type III and 3D models, leading to faster HUVEC migration, better adherence, and higher proliferation. The formation of a microvessel monolayer was also observed in these platforms contrasting with the absence of endothelization in 2D chips type III and 3D models (Figure 5b). These results showed the primary effect of the configurational differences between the models and fluid dynamics on HUVECs' motility and maturation.

The fluid dynamics in 2D chip types I, II, and III was estimated and compared through computational simulations using COMSOL Multiphysics software considering the transport of VEGF as a target molecule given its pivotal role in guiding the angiogenic sprouting of HUVECs. Computational studies predicted an average linear velocity of 2.0×10^{-7} m/s for 2D chip III slightly inferior to that estimated for 2D chip type I and II, of 6.7×10^{-7} m s^{-1} and 5.5×10^{-7} m s^{-1}, respectively (Figure 4a). The estimated linear velocities correlate well with the linear velocities obtained experimentally for the three different 2D models using fluorescent polystyrene beads (15 μm), as tracers, confirming the accuracy of the simulated values (Figure 4b).

Higher linear velocities in 2D chip types I and II may explain the improved migration of cells to the hydrogel chamber not only due to the higher associated shear stress but also because the higher velocity profiles in these models may render the development of more intense concentration gradients of cell nutrients and growth factors (e.g., VEGF) toward the gelatin chamber, therewith also guiding cell mobility in these platforms. HUVECs (Figure 5a) and MSCs migration observed in co-culture experiments (Figure 7b) seemed to be particularly dependent on VEGF concentration gradients, confirming the reported effect of VEGF-on guidance in angiogenic sprouting of HUVECs[32,33] and on-induced migration of MSCs to injury sites and hypoxic tissues.[34]

It is relevant to highlight that sprouting angiogenesis is conditioned by both the migration of endothelial progenitor cells to the injury site and by the release of VEGF to prompt endothelial progenitor cell proliferation and differentiation into a capillary.[35,36] Cell sprouting and endothelization were particularly evident in 2D chips type II but absent in 2D chips type III and 3D models (Figure 5b). The lack of efficient HUVECs maturation in 3D models may also be ascribed to an increased inner surface area of these models comparatively to 2D chips, resulting in a lower HUVECs density that may be insufficient to ensure ideal HUVEC sprouting and endothelization conditions.

Besides the relevancy of the geometrical configuration, the success of the 2D chip concept was also associated with the selective separation and entrapment of hydrogels containing the different cell cultures, i.e. MSCs encapsulated in mGelatin and HUVECs in Matrigel, on different compartments via capillary line pinning technique (Figure S1, Supporting Information) to avoid MSCs-HUVECs interactions (2D chips type I and II). As described in previous studies, the direct contact of MSCs and HUVECs could result in angiogenesis inhibition through

© 2023 Wiley-VCH GmbH

2365709x, 2023, 19, Downloaded from https://onlinelibrary.wiley.com/doi/10.1002/admt.202300617 by University Of Twente Finance Department, Wiley Online Library on [21/05/2024]. See the Terms and Conditions (https://onlinelibrary.wiley.com/terms-and-conditions) on Wiley Online Library for rules of use; OA articles are governed by the applicable Creative Commons License

the miR-211/Prox1 pathway[37] or cytotoxic effects of MSCs toward HUVECs.[38] Major cell death was observed in the regions where MSCs and HUVECs formed colonies after MSCs migration from the mGelatin compartment to the HUVECs reservoir (Figure 7b,d). Yet, the interaction between these colonies was minimized by the capillary barriers, as contemplated in 2D chip types I and II, with only 15% of HUVECs being accounted in the mGelatin compartment after 7 days (Figure 7d). Still, MSCs were able to efficiently mediate angiogenesis behavior on HUVECs (via paracrine mechanisms[39,40]) through the release of growth factors such as VEGF-A, confirming the MSC secretory activity widely reported in further literature,[41-43] and justifying the choice of MSCs for co-cultures on blood vessel models.

Several optimization strategies are based on different VEGF supplementation and cell seeding regimes to study which conditions are best to stimulate HUVEC maturation and vasculogenesis (Table S1 and Figure S5, Supporting Information). VEGF supplementation strategies showed some mild angiogenic improvement with endothelization appearing in scattered regions in the type I and II chips (Figures 5 and 6). More efficient angiogenic effects were obtained in type I and II chips by combining VEGF supplementation and multiple HUVEC seeding, resulting in cell sprouting observed by the presence of tube-like structures (Figure 6a). Still, only modest angiogenesis enhancement was achieved in 3D models, whereas a poor angiogenic effect was found in 2D chips type III, possibly ascribed to HUVECs encapsulation, resulting in limited access of HUVECs to nutrients and growth factors, or contact inhibition between MSCs and HUVECs cultured together. Metabolites analysis for 2D and 3D models over 7 days showed a healthy balance of glucose/ lactate concentrations of glucose above the critical value of 1 mM and lactate below toxic threshold of 10 mM, confirming cell viability throughout the experiments (Table S2, Supporting Information).

The importance of the access of cells to nutrients and factors was highlighted by the development of an LbL structure, which showed better performance on vasculogenesis development (Figure 6b) and the secretion of Endothelin-1 molecule, a marker of endothelialized matrix (Figure 8b). This result could be attributed to a higher volume of cell culture medium and nutrients in LbL, with increased contact area between cell compartments and fluid dynamics, leading to HUVECs stimulation and angiogenic sprouting.[44]

2D chips and 3D models containing MSC and HUVEC co-cultures were exposed to a 0.08 T static magnetic field between days 6 and 7. The increased angiogenic potential of MSCs growing on mGelatin by exposure to a low-intensity magnetic field was previously reported by the same authors.[23,24] The effect was ascribed to the stimulation of the paracrine activity of MSCs represented by VEGF release upon magnetically induced mechanotransduction. An identical effect may justify the positive influence of the magnetic force on the formation of a microvessel structure by HUVECs in 2D chips (Figure 8c) and 3D models, observed in the present work. The vasculogenesis of HUVECs was assessed by quantification of the endothelin-1 molecule expression, which was found to be boosted in the presence of the magnetic field. The Endothelin-1 release increase was higher in 2D chips, but still statistically significant for 3D models, showing that magnetic field stimuli (in models exposed to the magnetic field) are capable of supplanting the effect obtained by combined supplementary addition of VEGF and multiple cell seeding (in models not exposed to magnetic stimulation).

Magnetic stimulation was also found to induce the formation of microvessels and endothelialized matrix in the walls of the 3D models. This result is more significant in 3D veins than artery models, probably due to the lower wall thickness of vein models that facilitates molecule diffusion between outer and inner walls while enabling cell migration.

These novel approaches combine the use of magnetic field and magnetic-responsive hydrogels to provide more reliable and interpretative vascular models for in vitro cell studies. Also, these studies envision the potential use of magnetic stimulation for in situ regeneration of damaged/diseased blood vessels, which may pave the way for the discovery of novel treatments to reverse vascular ischemia conditions, such as cardiac ischemia.

4. Conclusions

Here we investigated the performance of 2D chips and 3D artificial arteries and veins, as vascularization platforms, capable of stimulating HUVECs maturation and angiogenesis, aiming their future application for vascular disease modeling. The vascularization models designed in this work were patterned with magnetic-responsive gelatin (mGelatin) containing encapsulated MSCs, which were used as a source of vascular growth factors, i.e. VEGF. The endogenous secretion of VEGF by MSCs encapsulated in the patterned mGelatin showed to be inefficient in assuring the desirable supply of VEGF in the absence of a magnetic field. However, when stimulated by a static magnetic field of 0.08 T for 24 h, the effect of the MSCs paracrine secretion on endothelization seemed to exceed the one obtained by VEGF daily supplementation, alone or combined with multiple HUVECs seeding. Indeed, magnetic stimulation boosted the formation of premature endothelialized tissue and microvasculature of co-cultures in both 2D chips (Type I and II) and 3D vein models. The best performance, regarding efficient microvessel formation, was obtained with 2D chips type I and II, as assessed by microtube counting and Endothelin-1 molecule quantification. These results may be explained by improved cell migration and adherence, potentially promoted by fluid dynamic conditions in 2D chips type I and II, which present higher linear velocities than type III, as predicted by COMSOL modeling studies. Improved sprouting effects were also achieved using 2D chips with layer-by-layer (LbL) configuration instead of those obtained by traditional fabrication methods, explained by the higher circulating volume of cell culture medium, thus resulting in higher cell numbers and cell nutrient amount in the chip.

3D models showed poorer angiogenic performances, in particular the artery models, potentially due to larger inner surface and the higher wall thickness, which may have hampered the establishment of the experimental conditions, such as ideal cell density and concentration gradients, that promote efficient cell migration and adhesion.

These results highlight the role of geometric configuration in vascularization platforms, its intrinsic fluid dynamics to regulate cell angiogenesis, and ultimately its importance for the

© 2023 Wiley-VCH GmbH

2365709x, 2023, 19, Downloaded from https://onlinelibrary.wiley.com/doi/10.1002/admt.202300617 by University Of Twente Finance Department, Wiley Online Library on [21/05/2024]. See the Terms and Conditions (https://onlinelibrary.wiley.com/terms-and-conditions) on Wiley Online Library for rules of use; OA articles are governed by the applicable Creative Commons License

2365709x, 2023, 19, Downloaded from https://onlinelibrary.wiley.com/doi/10.1002/admt.202300617 by University Of Twente Finance Department, Wiley Online Library on [21/05/2024]. See the Terms and Conditions (https://onlinelibrary.wiley.com/terms-and-conditions) on Wiley Online Library for rules of use; OA articles are governed by the applicable Creative Commons License

successful design of accurate in vitro vascular models. Furthermore, this work confirms the pro-angiogenic effect of static low-intensity magnetic field motivating the development of advanced magnetic field-based therapies for the regeneration of injured blood vessels for the treatment of several vascular-related diseases.

5. Experimental Section

Chips Fabrication: 2D chips were fabricated using polydimethylsiloxane polymer (PDMS, Dow Corning) following standard soft lithography techniques implemented in the MESA+ Institute at the University of Twente, The Netherlands.[12] Briefly, the chips were designed using Clewin software. The patterns were fabricated on silicon molds containing a SU-8 chip with the negative pattern. The SU-8 mold consisted of two 2100 SU-8 layers (Microchem): the first layer (450 µm height) contained the microstructures of the channels and reservoirs while the second layer (150 µm height) contained the capillary barriers (Figure 1). A Dektak surface profilometer (Bruker, Germany) was used to measure the SU-8 layers' average thicknesses. The PDMS chip was fabricated by casting a prepolymer (10:1 w/w ratio of PDMS and curing agent) on top of the SU-8 master of the silica wafers. After curing the prepolymer at 80 °C for 3 h, the PDMS layer was detached from the SU-8 master and cut into rectangular chips using a blade. The inlets and outlets for media perfusion were open in the PDMS layer using tissue punchers with 0.75 mm (media flow channels) and 3 mm (hydrogel channels) in diameter. The patterned surface of the PDMS layer was treated with oxygen plasma at 300 mTorr for 60 s using a Harrick Plasma Cleaner (PDC-32G, USA) and immediately bonded with an oxygen plasma-treated glass layer. The hydrogel patterning on the chip was performed 2–3 days after oxygen plasma bonding and the microchips were kept at−4 °C.

Magnetic Hydrogel Preparation: The magnetic hydrogel is composed of porcine skin gelatin (8% m/v, type A, G2500, Sigma-Aldrich) doped with magnetic nanoparticles (MNPs) - mGelatin was synthesized by chemical co-precipitation of iron salts $FeCl_3$ and $FeCl_2$ (Sigma-Aldrich) in alkaline media, according to the protocol published by Izquierdo et al.[45] MNPs were dried in ethanol solution at room temperature to form a magnetic powder. Porcine skin gelatin was dissolved in Milli-Q water (10% m/v) at 60 °C. Powder MNPs were dispersed by sonication and mixed with gelatin polymeric aqueous solution to form a homogeneous solution. The solution was maintained at −20 °C to prevent fungi contamination on the gelatin.

Magnetic Hydrogel Patterning on 2D Chips: Before hydrogel patterning in the chips, the solution of gelatin and MNPs was heated at 70 °C to ensure reduced viscosity and avoid clogging issues. Immediately after heating, 1% of glutaraldehyde (v/v) (Sigma Aldrich) was added to the mixture for gelatin crosslinking and the patterning process occurred via capillary action (Figure 1). Excess hydrogel solution was removed to ensure that the hydrogel mixture remained between the endothelial cell reservoirs and the media microchannels due to the capillary pinning process. The chips were placed at −20 °C before cell culture experiments to allow for hydrogel curing while avoiding the formation of air bubbles and hydrogel leakage to other compartments. Before seeding the cells, the magnetic coating was washed by perfusion of PBS solution (Phosphate Buffered Saline, Sigma Aldrich) three times to remove unbonded components. The samples were sterilized by perfusion of a PBS solution containing 1% antibiotic-antimycotic (Gibco) for 3 h. The cells were pre-conditioned by immersions in DMEM cell culture medium (Dulbecco's Modified Eagle Medium, ThermoFisher Scientific) for 3 h before perfusion through the media flow microchannels. The tubing and the microfluidic connectors used in the experiments were sterilized by rinsing with 70% (v/v) ethanol and then with PBS solution. Matrigel (Corning, NY) was additionally patterned on the HUVECs compartment of Types I and II. In this case, a thin layer of Matrigel was coated in the bottom of the microchips to allow for HUVECs' support. The Matrigel excess was carefully removed from the channel with a syringe pump and the HUVECs culture was seeded on top of the Matrigel coating.

Constructs Fabrication: 3D single-channel blood vessels were fabricated following molding techniques. Silicone tubing was used as molds to fabricate models of large arteries and veins. Initially, the tubing was coated with a solution of Gel Slick solution (Lonza) for surface treatment, to allow for easier demolding and air drying before use. The molding setup (Figure 2a) consisted of a smaller tubing inserted within a larger one and glued to plastic support according to the desired artery and vein model dimensions. The space in between the tubing was then filled with the magnetic-responsive gelatin solution and placed at 4 °C for gelation overnight. The outer tubing was then cut and removed while the sample was still cold, and the inner tubing was gently demolded. The 3D molds were immersed in a solution containing 3% of Glutaraldehyde for crosslinking for 3 h. To remove unbound material, the molds were washed twice with PBS solution and sterilized using a PBS solution containing 1% antibiotic-antimycotic for 3 h. The molds were stored at −20 °C and pre-conditioned with a cell culture medium (DMEM) before use.

mGelatin Mechanical Characterization: Compression mechanical testing was performed before and after the addition of the crosslinking agent, with an Instron Tensile Compression equipment at Elastomer Technology, as described in detail in Section S8 (Supporting Information).

Cell Culture: Human bone-marrow MSCs (BM-hMSCs) here used were obtained from the cell bank of Stem Cell Engineering Research Group (SCERG), iBB-Institute for Bioengineering and Biosciences at Instituto Superior Técnico (IST). Bone marrow aspirates were obtained from Instituto Português de Oncologia Francisco Gentil, Lisboa-Portugal under collaboration with iBB-IST. All human samples were obtained from healthy donors after written informed consent, according to Directive 2004/23/EC of the European Parliament and of the Council of 31 March 2004 on setting standards of quality and safety for the donation, procurement, testing, processing, preservation, storage, and distribution of human tissues and cells (Portuguese Law 22/2007, June 29), with the approval of the Ethics Committee of the respective clinical institutions.[46] Isolated cells were cryopreserved in liquid/vapor nitrogen tanks until further use. Isolated BM-hMSCs were cultured using low-glucose supplemented with 10% fetal bovine serum (FBS MSC qualified, Gibco) and 1% antibiotic-antimycotic and kept at 37 °C, 5% CO_2, and 21% O_2 in a humidified atmosphere. HUVECs were purchased from Lonza (Basel, Switzerland) and maintained in commercial endothelial growth medium-2 (EGM-2, Lonza) at 37 °C, 5% CO_2 in a humidified atmosphere. Media renewal was performed every 3–4 days. All the experiments were performed using cells between passages 4 and 7.

Co-Culture of MSCs and HUVECs and Magnetic Stimulation: *2D Chips*: MSCs (seeding density of $1.5x10^6$ cells/mL) were perfused on day 1 through the chips media channels and allowed to migrate and adhere to the magnetic hydrogel overnight. Some inlets were also punched on the PDMS layer above the hydrogel compartment, allowing for MSCs injection (1 µL) in those specific regions to boost cell proliferation (Figure 1a). Matrigel solution was also perfused on the endothelial cell compartment as cell growth support while HUVECs (seeding density of 3×10^6 cells mL^{-1}) were seeded by perfusion directly to the compartment on day 2. A syringe pump was connected to the media flow inlets of the chips (Figure 1a) and a volumetric flow of 300 µL h^{-1} was set to infuse cell culture media in the media flow channels. The outlets of the chips were connected to a recipient and the depleted stream was collected every day for further analysis. The syringes were replaced with fresh medium every day, containing DMEM + 10% FBS and EGM-2 in a 1:1 proportion.

3D Models: Followed the same cell density, volumetric flow, cell culture medium, and perfusion conditions as 2D chips. However, the 3D model was placed in a petri dish immersed in a cell culture medium and supported as shown in Figure 2b. MSCs were seeded manually in the outer wall of the 3D models on day 1 and allowed to adhere for 24 h. HUVECs were seeded in the lumen (inner wall of the model) on day 2, with a volumetric flow of 300 µL h^{-1}. The media was collected every day for further analysis and replaced with fresh medium.

All experiments with 2D and 3D models were performed in incubators at 37 °C in 5% CO_2 in a humidified atmosphere under normoxia conditions, for 7 days. A neodymium magnet was placed beneath the chips

 © 2023 Wiley-VCH GmbH

for the last 24 h (day 6) allowing magnetic stimulation with an intensity of 0.08 T.

VEGF and Endothelin-1 Measurement using ELISA: VEGF-A and Endothelium-1 were quantified using the Human VEGF-A kit (RayBiotech) and Endothelium-1 kit (RayBiotech), respectively, according to manufacturer instructions. All conditions were tested in triplicates using the same MSC donor to avoid further variability in the results.

Morphological Analysis: Cell viability using calcein staining (Live & Dead kit, Invitrogen) was recorded throughout experiments using an EVOS FL imaging system equipped with a GFP filter cube. The cytoplasm of HUVECs was fixed with 4% (v/v) of paraformaldehyde (Sigma Aldrich) and permeabilized in 0.1% (v/v) Triton X-100 (Sigma Aldrich) for 10 min and cell nuclei were stained using DAPI (Sigma Aldrich), Yo-Yo and Ethidium Bromide (ThermoFisher Scientific, USA) for analysis by laser scanning confocal microscope (Zeiss LSM 510, Germany). Live and Dead images were obtained using combined Calcein and Ethidium Bromide staining (LIVE/DEADTM Viability/ Cytotoxicity Kit, for mammalian cells, ThermoFisher Scientific) after 20 min of incubation with MSCs and HUVECs co-culture using a fluorescence microscope (Leica DM IL LED with EC3 camera system).

CD31 Immunostaining: HUVECs immune-characterization was carried out using CD31 antibody after the co-culture (MSCs and HUVECs) fixation with 4% paraformaldehyde and blocking with 10% FBS (Fetal Bovine Serum, Gibco) in PBS solution. Primary antibody CD31 (1:50 dilution, mouse antibody, Dako) in block solution was perfused in the chips and incubated overnight. The secondary antibody Alexa 546 (1:500 dilution, goat anti-mouse, Abcam) was added to the chips and incubated for 30 min. Images were obtained using a fluorescence microscope (Leica DM IL LED with EC3 camera system) and a confocal laser scanning microscope (LSM 700/ Carl Zeiss).

Statistical Analysis: All measurements were performed twice, under independent conditions. Two-way ANOVA Sidak's multiple comparisons test was used to compare the mean of three values obtained from three independent conditions in ELISA assay, using GraphPad Prism version 7 (GraphPad Software, La Jolla, CA); $*p < 0.05$ indicates a significant result; $**p < 0.01$ a very significant result, $***p < 0.001$ a highly significant result, and $****p < 0.0001$ an extremely significant result.

Supporting Information

Supporting Information is available from the Wiley Online Library or from the author.

Acknowledgements

The authors acknowledge the financial support from Fundação para a Ciência e a Tecnologia (FCT-MEC), Portugal, through the dedicated project [PTDC/EDM-EDM/30828/2017] (BeLive), the Ph.D. grant [SFRH/BD/114043/2015] and the research units REQUIMTE [UIDB/50006/2020 and UIDP/50006/2020], iBB [UIDB/04565/2020] and i4HB (LA/P/0140/2020). The authors also acknowledge the financial support of Institute of Complex Molecular Systems at Eindhoven University of Technology.

Conflict of Interest

The authors declare no conflict of interest.

Author Contributions

A.C.M., C.AM.P., F.C.F., B.G., and H.G. performed conceptualization. A.C.M., B.G., and F.C.F. performed methodology. A.C.M. performed data analysis. A.C.M. prepared the original draft. All the authors wrote, review, and edited the draft. C.A.M.P., F.C.F., B.G., and H.G. performed supervision. C.A.M.P., F.C.F, and H.G. performed funding acquisition. All authors reviewed the final manuscript.

Data Availability Statement

The data that support the findings of this study are available on request.

Keywords

3D molding designs, angiogenesis, blood vessels, human umbilical vein endothelial cells, magnetic field, mesenchymal stromal cells, microfluidic technology

Received: April 22, 2023
Revised: June 28, 2023
Published online: September 5, 2023

[1] S. Abhishek, *Lab Chip* **2019**, *19*, 2500.
[2] M. B. Bracken, *J R Soc Med* **2009**, *102*, 120.
[3] T. Matsumoto, S. Sugita, T. Yaguchi, *Advances in Metallic Biomaterials*, Springer, New York **2015**, 71.
[4] A. Hasan, A. Paul, A. Memic, A. Khademhosseini, *Biomed. Microdevices* **2015**, *17*, 88.
[5] E. Gagnon, P. Cattaruzzi, M. Griffith, L. Muzakare, K. LeFlao, R. Faure, R. Béliveau, S. N. Hussain, M. Koutsilieris, C. J. Doillon, *Angiogenesis* **2002**, *5*, 21.
[6] Q. Smith, S. Gerecht, *Curr. Opin. Chem. Eng.* **2014**, *3*, 42.
[7] A. K. Miri, B. Cecen, A. Khademhosseini, A. Khalilpour, S. R. Shin, S. Maharjan, *Biomaterials* **2018**, *198*, 204.
[8] S. Kim, W. Kim, S. Lim, J. S. Jeon, *Bioengineering* **2017**, *4*, 8.
[9] D. T. Chiu, A. J. deMello, D. Di Carlo, P. S. Doyle, C. Hansen, R. M. Maceiczyk, R. C. R. Wootton, *Chem* **2017**, *2*, 201.
[10] S. Kim, H. Lee, M. Chung, N. L. Jeon, *Lab Chip* **2013**, *13*, 1489.
[11] I. S. Kinstlinger, G. A. Calderon, M. K. Royse, A. K. Means, B. Grigoryan, J. S. Miller, *Nat. Protoc.* **2021**, *16*, 3089.
[12] Y. Tsukamoto, T. Akagi, M. Akashi, *Sci. Rep.* **2020**, *10*, 5484.
[13] B. Gumuscu, A. S. Haase, A. M. Benneker, M. A. Hempenius, A. van den Berg, R. G. H. Lammertink, J. C. T. Eijkel, *Adv. Funct. Mater.* **2016**, *26*, 8685.
[14] B. Gumuscu, H. J. Albers, A. Van Den Berg, J. C. T. Eijkel, A. D. Van Der Meer, *Sci. Rep.* **2017**, *7*, 1.
[15] M. P. Tibbe, A. M. Leferink, A. van den Berg, J. C. T. Eijkel, L. I. Segerink, *Adv. Mater. Technol.* **2018**, *3*, 1.
[16] J. R. Ferreira, G. Q. Teixeira, S. G. Santos, M. A. Barbosa, G. Almeida-Porada, R. M. Gonçalves, *Front Immunol* **2018**, *9*, 2837.
[17] K. E. Johnson, T. A. Wilgus, *Adv Wound Care* **2014**, *3*, 647.
[18] M. Schubert, H. Friess, J. Mattern, G. Moldenhauer, W. Wagner, A. Apel, R. Saffrich, A. D. Ho, P. Büchler, I. Herr, N. Giese, A. Diehlmann, M. W. Büchler, D. Frommhold, A. V. Salnikov, G. Kallifatidis, B. M. Beckermann, A. Groth, *Br. J. Cancer* **2008**, *99*, 622.
[19] Q. Ge, H. Zhang, J. Hou, L. Wan, W. Cheng, X. Wang, D. Dong, C. Chen, J. Xia, J. Guo, X. Chen, X. Wu, *Mol. Med. Rep.* **2018**, *17*, 1667.
[20] X. Wang, Q. Sun, J. Pei, *Micromachines* **2018**, *9*, 493.
[21] A. C. Manjua, V. D. Alves, J. G. Crespo, C. A. M. Portugal, *ACS Appl. Mater. Interfaces* **2019**, *11*, 21239.
[22] A. C. Manjua, J. M. S. Cabral, C. A. M. Portugal, F. C. Ferreira, *Sci. Technol. Adv. Mater.* **2021**, *22*, 461.
[23] A. C. Manjua, J. M. S. Cabral, F. C. Ferreira, C. A. M. Portugal, *Polymers (Basel)* **2021**, *13*, 1883.
[24] J. S. Jeon, S. Bersini, J. A. Whisler, M. B. Chen, G. Dubini, J. L. Charest, M. Moretti, R. D. Kamm, *Integr. Biol.* **2012**, *100*, 130.
[25] B. Gumuscu, J. C. T. Eijkel, *Methods Mol Biol* **2018**, *1771*, 225.
[26] O. Traub, B. C. Berk, *Arterioscler., Thromb., Vasc. Biol.* **1998**, *18*, 677.
[27] V. Der Vosse, Cardiovascular Fluid Mechanics pp 51–61.

© 2023 Wiley-VCH GmbH

2365709x, 2023, 19, Downloaded from https://onlinelibrary.wiley.com/doi/10.1002/admt.202300617 by University Of Twente Finance Department, Wiley Online Library on [21/05/2024]. See the Terms and Conditions (https://onlinelibrary.wiley.com/terms-and-conditions) on Wiley Online Library for rules of use; OA articles are governed by the applicable Creative Commons License

[28] R. Akhtar, M. J. Sherratt, J. K. Cruickshank, B. Derby, *Mater. Today* **2011**, *14*, 96.
[29] L. Laurent, L. B. Fabrice, H. Jacques, *Circ. Res.* **2007**, *100*, 782.
[30] F. L. Marasciulo, M. Montagnani, M. A. Potenza, *Curr. Med. Chem.* **2006**, *13*, 1655.
[31] D. Wang, Y. Xu, Q. Li, L. S. Turng, *J. Mater. Chem. B* **2020**, *8*, 1801.
[32] L. Liu, B. D. Ratner, E. H. Sage, S. Jiang, *Langmuir* **2007**, *23*, 11168.
[33] H. Gerhardt. *VEGF and Endothelial Guidance in Angiogenic Sprouting BT – VEGF in Development*, (Ed.: C. Ruhrberg), Springer New York, New York, NY **2008**, pp 68–78.
[34] C. Ke, J. Chen, Y. Guo, Z. W. Chen, J. Cai, *Biochim. Biophys. Acta – Biomembr.* **2015**, *1848*, 859.
[35] M. D. Sarker, S. Naghieh, N. K. Sharma, X. Chen, *J Pharm Anal* **2018**, *8*, 277.
[36] J. Pauty, I. G. Cheng, Y. T. Matsunaga, E. Lee, M. Kobayashi, L. Hespel, F. Yger, K. Kato, F. Soncin, H. Nakajima, H. Takahashi, R. Usuba, *EBioMedicine* **2017**, *27*, 225.
[37] J. Pan, X. Wang, D. Li, J. Li, Z. Jiang, *J. Biochem.* **2019**, *166*, 107.
[38] K. Otsu, S. Das, S. D. Houser, S. K. Quadri, S. Bhattacharya, J. Bhattacharya, *Blood* **2009**, *113*, 4197.
[39] L. Brewster, S. Robinson, R. Wang, S. Griffiths, H. Li, A. Peister, I. Copland, T. McDevitt, *J Vasc Surg Venous Lymphat Disord* **2017**, *65*, 826.
[40] M. R. Javan, A. Khosrojerdi, S. M. Moazzeni, *Front Oncol* **2019**, *9*, 840.
[41] Q. Ge, H. Zhang, J. Hou, L. Wan, W. Cheng, X. Wang, D. Dong, C. Chen, J. Xia, J. Guo, X. Chen, X. Wu, *Mol. Med. Rep.* **2018**, *17*, 1667.
[42] S. Y. Ahn, W. S. Park, Y. E. Kim, D. K. Sung, S. I. Sung, J. Y. Ahn, Y. S. Chang, *Exp. Mol. Med.* **2018**, *50*, 26.
[43] H. Tao, Z. Han, Z. C. Han, Z. Li, *Stem Cells Int* **2016**, *2016*, 1314709.
[44] P. A. Galie, D.-H. T. Nguyen, C. K. Choi, D. M. Cohen, P. A. Janmey, C. S. Chen, *Proc. Natl. Acad. Sci. USA* **2014**, *111*, 7968.
[45] Á. Cruz-Izquierdo, E. A. Picó, C. López, J. L. Serra, M. J. Llama, *PLoS One* **2014**, *9*, e105620.
[46] F. Dos Santos, P. Z. Andrade, J. S. Boura, M. M. Abecasis, C. L. Da Silva, J. M. S. Cabral, *J. Cell. Physiol.* **2010**, *223*, 27.

© 2023 Wiley-VCH GmbH

2365709x, 2023, 19, Downloaded from https://onlinelibrary.wiley.com/doi/10.1002/admt.202300617 by University Of Twente Finance Department, Wiley Online Library on [21/05/2024]. See the Terms and Conditions (https://onlinelibrary.wiley.com/terms-and-conditions) on Wiley Online Library for rules of use; OA articles are governed by the applicable Creative Commons License